Energy Deposition in APS-U Whole-Beam Dumps

J. Dooling, M. Borland, B. Micklich

Argonne National Laboratory, 9700 S. Cass Avenue, Argonne, IL 60559

Argonne National Laboratory is a U.S. Department of Energy laboratory managed by U Chicago Argonne, LLC.

7^{th} **HPTW P74**

Abstract

The Advanced Photon Source Upgrade (APS-U) will generate high-brightness x-rays using small, intense, 6-GeV electron beams with transverse dimensions of 0.010-0.015 mm, rms. Full beam aborts in the APS-U storage ring will sometimes be required for machine and personnel protection. These involve removing power from the accelerating cavities, which allows the beam to spiral in until it hits a whole beam dump (WBD). Simulations with MARS [1] show that any solid material subject to a full beam abort (720 nC, 6 GeV) will be damaged and pushed into a hydrodynamic regime (>15 MGy). As a result, the WBD must be repositioned after each full beam abort to expose new surface. Aside from choosing the appropriate material, an understanding of how the material behaves during the beam abort is required both for personnel and machine protection. A significant change to the WBD density during a beam abort will modify its ability to absorb energy during the later stages of the loss event. As examples, we evaluate the dose in four candidate materials: aluminum, titanium alloy, copper, and tungsten. We show that static simulations coupled with simple back-of-the-envelope calculations strongly suggest the generation of shocks in high-density, high-Z materials, likely making them unsuitable for the WBD. The need to couple a hydrodynamics code with the static dose simulation is discussed.

Outline

- Beam Damage Experienced in the APS Storage Ring
- Whole Beam Loss Considerations for the APS-U Dump/Collimators
- Summary and Future Work

Beam Damage

We see e-beam damage to S37 horizontal scraper in the present APS SR. Energy density in the upgrade (APS-U) will be much higher.

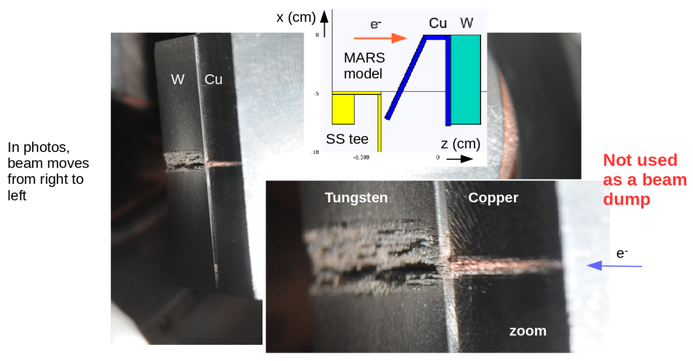

Figure 1: *Diagnostic scraper damage discovered in 2011.*

Experimental scraper testing April 2012—last day of the run

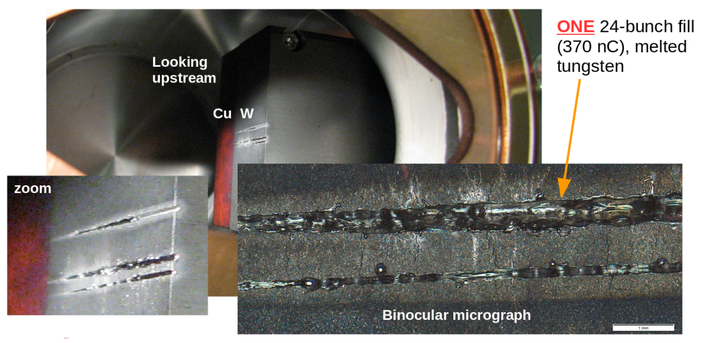

Figure 2: *Experimental scraper damage observed after 1 run.*

The experimental scraper was left out of the beam path for the entire 2012-1 Run and inserted only on the last day of the run. The beam was intentionally dumped at varying heights on the scraper using different fill patterns. Of particular interest were the hybrid (1 large singlet, 18 mA) and the 24-bunch (4.2 mA) fill patterns.

Simulations for APS-U Whole-Beam Dump

Beam loss distributions are calculated with `elegant` [2] then used as input to MARS [1]. The beam energy is 6 GeV; total charge is 720 nC (4.6×10^{12} electrons). High resolution dose distributions are recorded in a 0.02 mm x 0.02 mm x 10 mm Cartesian grid in the central square mm about the beam location.

Simplified Geometry in MARS for dump collimator and nearby magnet

Have settled on matched cylindrical surfaces to minimize impedance

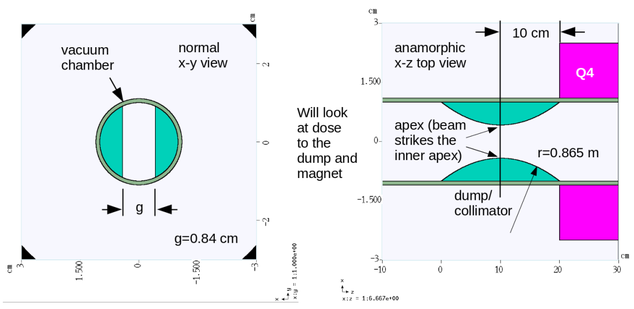

Figure 3: *Beam Dump-Collimator Geometry in MARS. The imaage on the right is a shows a plan (top) x-z view cut through the geometry at beam elevation (y=0)*

Beam will first strike the inboard apex of the collimator moving from left to right. The electromagnetic shower then develops downstream. The following images show the electron-positron fluence generated after the beam strikes collimator. In the next 4 images, the collilmator material is modeled with aluminum, titanium alloy (TiAlV), copper, and tungsten.

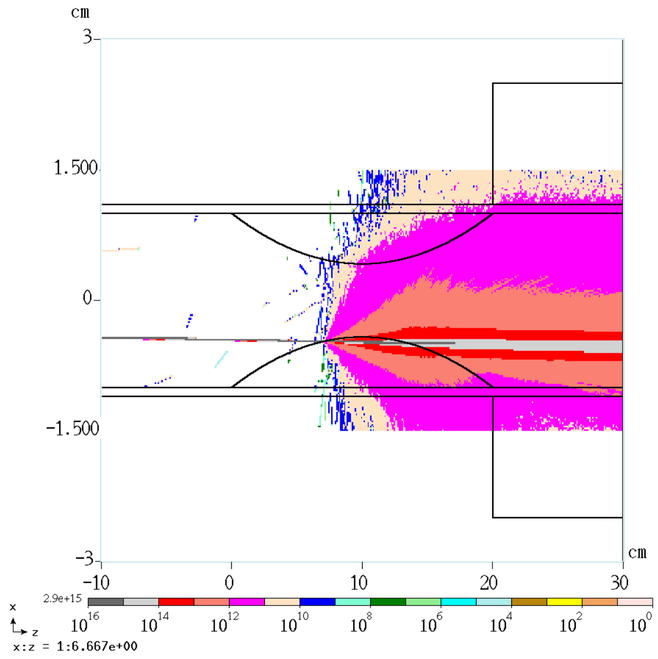

Figure 4: *Aluminum.*

Peak Power P and Power density, P_d in a single bunch of 48, each 92 J
$\sigma_x = 0.024$ mm, $\sigma_y = 0.0065$ mm, $\sigma_t = 100$ ps
$P = E/(2\sqrt{2\ln(2)}\sigma_t) = 3.91\times10^{11}$ W
$P_d = P/(8\pi\ln(2)\sigma_x\sigma_y) = 1.13\times10^{14}$ W/mm^2.

Note the model is static; i.e., the target material does not move or change phase regardless of the received dose. These x-z figures present an anamorphic view, compressed in z (Aspect ratio: 6.667 to 1).

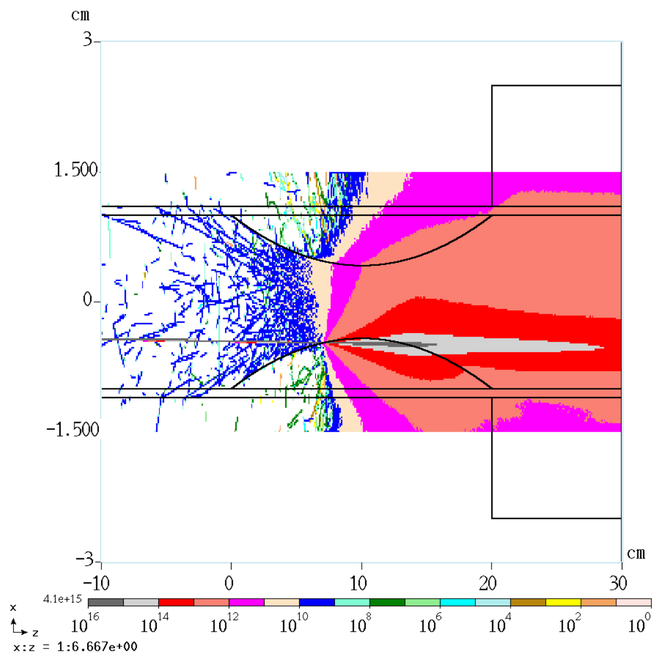

Figure 5: *Titanium alloy.*

The increased density and higher Z of titanium spreads the shower farther transversely relatively to aluminum.

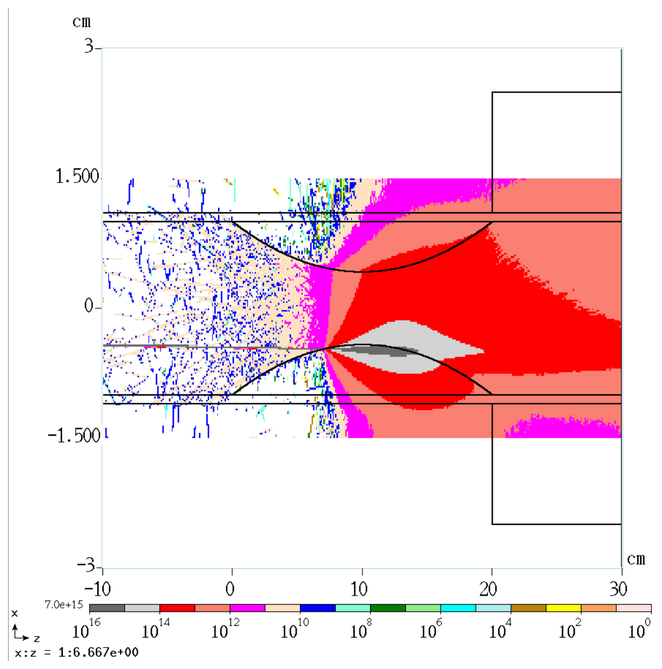

Figure 6: *Copper.*

Copper sends a larger fraction of the shower toward the outboard wall and magnet region; hydrodynamic effects[3] may modify this picture.

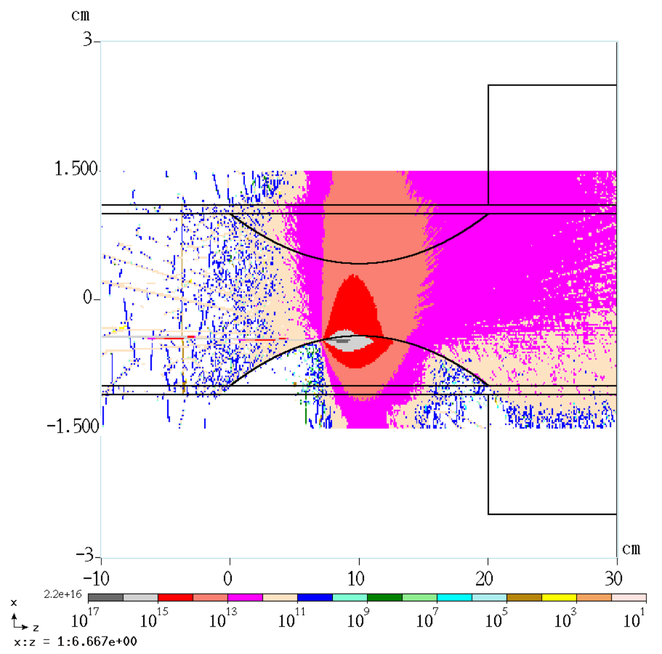

Figure 7: *Tungsten. Subject to hydrodynamic modification.*

Tungsten appears to be best at stopping the beam; however, the short radiation length ($X_o/\rho = 3.56$ mm) and high energy density indicates shocks and hydrodynamic tunneling would likely lead to significant damage of the collimator and increased DS shower.

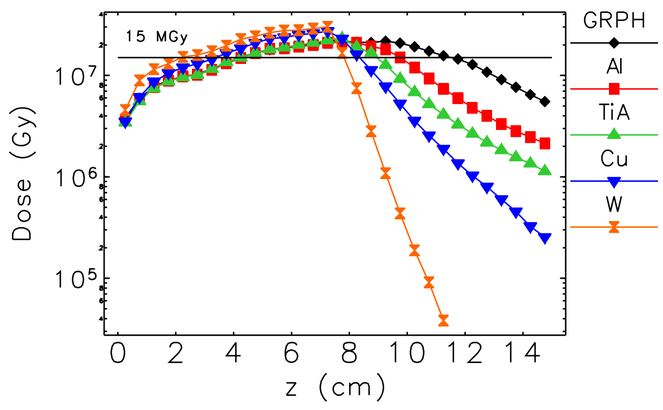

Figure 8: *Whole beam dose vs. distance in various materials. In all cases, peak dose exceeds 15 MGy which roughly defines the hydrodynamic regime boundary.*

Dose and Temperature Rise

The peak energy density in the beam is

$$E_d = \frac{N_e m_e c^2 \gamma}{2\pi\sigma_x\sigma_y}, \qquad (1)$$

where N_e is the number of electrons, and σ_x (σ_y) is the horizontal (vertical) rms beam size. Ignoring phase transitions and assuming constant heat capacity, the temperature rise is

$$\Delta T = \frac{D A_w}{C_m}, \qquad (2)$$

where D is the dose (J/kg or Gy), A_w is the atomic weight (kg/mole), and C_m is the molar specific heat (J/K/mole).

$$D = S_{pc}\frac{N_e}{2\pi\sigma_x\sigma_y}, \qquad (3)$$

where S_{pc} is the collisional stopping power, which gives the ionization energy loss into ionization and directly results in heating.

The NIST database gives values for S_{pc} [4].

The following transverse (x-y) views show the absorbed dose at z=25 cm, a location within the Q4 magnet. Only the results for Al and Ti-alloy are presented here; we believe hydrodynamic effects will alter the results in the cases of copper or tungsten collimators.

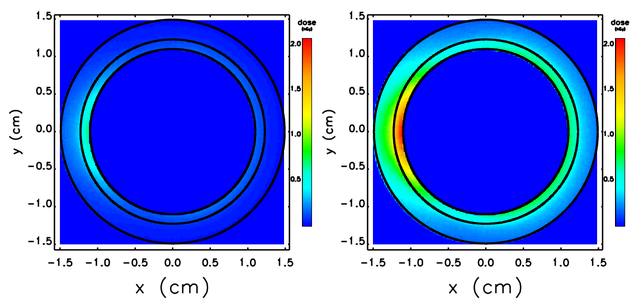

Figure 10: *Whole beam dose downstream of the collimator for Al and Ti-alloy.*

In the case of a titanium-alloy collimator, peak dose of 1.2 kGy is predicted in the magnet region closest to the vacuum chamber; this level drops to 0.4 kGy for an aluminum collimator.

The following table compares peak thermal-to-yield stresses and expansion rates to acoustic velocities, in the case of a single 15.3-nC, 6-GeV bunch. Transverse bunch rms dimensions are 24 μm horizontally by 8 μm vertically.

$g = \frac{\sigma_T}{\sigma_Y} = \frac{\alpha E_Y \Delta T}{\sigma_Y}$ $\quad d_\alpha = \alpha r_b \Delta T$ $\quad$ $\sigma_{T(Y)}$: thermal (yield) stress, E_Y: Young's modulus

mat'l.	$\alpha\times10^6$ (K^{-1})	d_α (μm)	E_Y (GPa)	σ_Y (MPa)	σ_T (MPa)	g	v_{ac}* (m/s)	v_α (m/s)	g_v
Al	23.1	1.04	70	310	3693	10.32	5000	4165	0.83
TiA	8.6	0.60	116	951	3445	3.62	5090	2400	0.47
Cu	16.5	1.78	110	220	8874	40.33	3810	7132	1.87
W	4.5	2.02	345	1510	26,040	17.25	4620	8087	1.75

`elegant` simulations indicates a 48-bunch whole beam dump will deposit roughly 60 percent of its energy in 10 turns (≈ 37 μs). The plot below shows the number of macroparticles lost per Pass or turn in APS-U after the rf is switched off at turn 10,000. The SR beam begins to strike the wall after approximately 55 turns. Also presented is the cumulative fraction of particles lost vs turn.

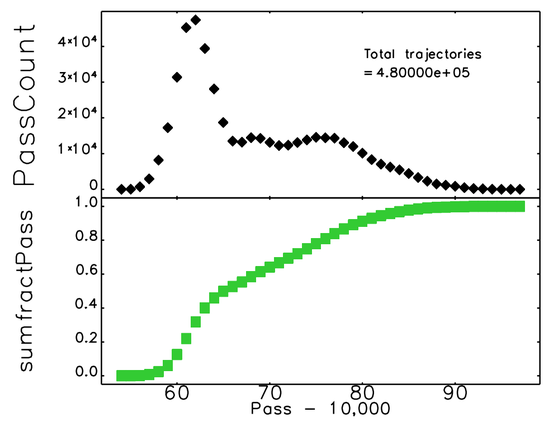

Figure 12: *Whole beam dump loss per Pass*

Beam Strike on Dump/Collimator

- Low-Z metals (e.g. aluminum) are probably the best choice for the dump/collimator (TiA second choice)
- An aluminum collimator yields the smallest dose locally in wall and magnet; smallest temperature rise
- Al produces the least activation
- Al is the same material as surrounding vacuum chamber wall
- Need to examine the scattered beam downstream of the dump/collimator
- Temporal behavior and fill pattern are important for thermal diffusion considerations

Summary and Further Work

- Must protect the machine from whole beam dumps
- Dump/collimator will be damaged—sacrificial, move after each beam dump
- Need hydrodynamics code to assess hydrodynamic tunneling and actual dose downstream of the collimators
- Low-Z metal (probably Al) is the best candidate for the dump/collimator
- Conduct tests where possible to bench-mark simulations

Acknowledgments

Thanks to R. Soliday for assistance with analyis scripts.

References

[1] N. V. Mokhov, et al. Fermilab-Conf-07/008-AD; AIP Conf. Proc. 896, FNAL (2007).

[2] M. Borland. ANL/APS LS-287, Advanced Photon Source (2000).

[3] N. Tahir, et al. *Nuclear Inst, and Methods in Physics Research B*, 427:70 (2018).

[4] NIST e-star database. https://physics.nist.gov/PhysRefData/Star/ Text/ESTAR.html.